

Article ID: 1009-637X(2001)01-0014-10

Estimation of net primary productivity in China using remote sensing data

SUN Rui, ZHU Qi-jiang

(Dept. of Resources and Environment Sciences, Beijing Normal University, Beijing 100875, China)

Abstract: It is significant to estimate terrestrial net primary productivity (NPP) accurately not only for global change research, but also for natural resources management to achieve sustainable development. Remote sensing data can describe spatial distribution of plant resources better. So, in this paper an NPP model based on remote sensing data and climate data is developed. And 1km resolution AVHRR NDVI data are used to estimate the spatial distribution and seasonal change of NPP in China. The results show that NPP estimated using remote sensing data are more close to truth. Total annual NPP in China is 2.645×10^9 tC. The spatial distribution of NPP in China is mainly affected by precipitation and has the trend of decreasing from southeast to northwest.

Key words: remote sensing, net primary productivity, vegetation, model, seasonal change

CLC number: X87; P935.1; Q948 **Document code:** A

1 Introduction

As a major part of terrestrial ecosystem, vegetation plays an important role in the energy, matter and momentum exchange between land surface and atmosphere. Through the process of photosynthesis, land plants assimilate carbon in atmosphere and incorporate into dry matter while part of carbon is emitted into atmosphere again through plant respiration. The remainder of photosynthesis and respiration is called net primary productivity (NPP), which is important in the global carbon budget. Humans and other animals are dependent on a fraction of NPP for food, fuel and fiber. Therefore, to estimate NPP accurately not only can help us to understand global carbon cycle, it is also significant for natural resources management to achieve sustainable development.

There are now three kinds of NPP model mainly^[1]: climate model, process model and energy use efficiency model. Climate model estimate NPP by establishing the statistical relation between NPP and climate data^[2-4]. For example, Miami model uses empirical relationship between NPP, annual mean temperature and precipitation to estimate global terrestrial NPP^[2]. However, this kind of model doesn't consider actual land vegetation type, and the estimated NPP is trend or potential NPP, so there exists great difference between estimated NPP and ground truth.

Process model estimates NPP based on plant physiological and ecological processes, such as BEPS^[5], DEMETER^[6], FOREST-BGC^[7]. Because process models considered many processes such as photosynthesis, plant respiration and dry matter partition, there are many parameters in these models.

Received date: 2000-08-26 **Accepted date:** 2000-10-15

Foundation item: National Natural Science Foundation of China, No. 49871055; No. 39990490; key basic research project of China, No. 95-Y-38

Author: Sun Rui (1970-), Ph.D., Lecturer, specialized in vegetation study by remote sensing. E-mail: rui-sun@263.net

However, because many parameters and some variables that change with phenology are difficult to determine, we have to specify these parameters or simplify the model.

Recently, the availability of multi-temporal and multi-spectral remote sensing information has enabled measurement and monitoring land surface parameters such as leaf area index, phenology and fraction of absorbed photosynthetic active radiation (FPAR) by vegetation, which will help us to study the spatial distribution, seasonal and inter-annual change of NPP. Especially the AVHRR sensor on NOAA satellite provides daily, global, red and near-infrared reflectance data, from which cloud-free, near nadir composite data can be formed at a frequency of once every month. So NOAA-AVHRR data has been widely used to estimate plant production. Because there exists a near-linear relationship between FPAR and vegetation index, especially simple ratio ($SR=NIR/VIS$, NIR and VIS are the reflectance at near infrared band and visible band) and normalized difference vegetation index ($NDVI=(NIR-VIS)/(NIR+VIS)$), SR and NDVI have been used to determine FPAR^[8-10]. Energy use efficiency model uses energy use efficiency and the relationship between vegetation index and FPAR to estimate NPP. Because energy use efficiency model is simple and uses remotely sensed data, it has been widely used.

In this paper, first we develop a NPP model based on remote sensing data and climate data. And then using this model and 1km resolution monthly AVHRR NDVI data, the spatial distribution and seasonal change of NPP in China are analyzed.

2 Data and pre-processing

In the study, we use monthly 1km resolution AVHRR NDVI data from June 1992 to March 1993. The NDVI data come from 1km resolution NOAA-AVHRR NDVI data set created by Earth Resources Observation Systems Data Centre and United States Geological Survey^[11]. The projection of image is Lambert azimuth equal area projection. In order to get cloud free data, the monthly NDVI data was created by maximizing value composite method, that is to select the max NDVI value in the month as monthly NDVI value in every pixel^[11]. Because some parameters in the model are dependent on vegetation type, we have used the multi-temporal NDVI data and maximized likelihood classification to get the vegetation map of China.

In order to calculate soil water content, the Map of Soil Texture of China^[12] is digitized and converted into 1km resolution grid data using ARC/INFO software. At the same time, the climate data include monthly precipitation, air temperature, wind speed, vapor pressure and percentage of sunshine from April 1992 to March 1993 are also interpolated to 1km resolution grid data using Kriging method.

3 Model description and structure

3.1 Model description

In the energy use efficiency model, NPP is estimated by energy conversion efficiency and the photosynthetic active radiation absorbed by vegetation (APAR). Prince *et al.* proposed that in order to estimate NPP more accurately, not only the effect of environmental factors on dry matter production should be considered, but also plant respiration should be considered. They demonstrated that the maximum energy use efficiency of gross primary productivity (GPP) is more stable than that of NPP, which doesn't change much with climate, plant type and soil water condition^[10]. So in this paper, we divide NPP into two parts: GPP and respiration, that is

$$NPP=GPP-R \quad (1)$$

where NPP , GPP and R represent net primary productivity, gross primary productivity and respiration respectively ($gCm^{-2}month^{-1}$).

GPP is computed by energy use efficiency model:

$$GPP = \varepsilon_g^* \times f_1(T) \times f_2(\beta) \times FPAR \times PAR \quad (2)$$

in which ε_g^* is maximum energy conversion efficiency, it equals to 2.76g/MJ; $f_1(T)$ and $f_2(\beta)$ are the influential factors of temperature and soil water content on ε_g^* ; T is air temperature (°C); β is evaporation rate, which is the ratio of actual evapotranspiration and potential evapotranspiration; and FPAR is fraction of photosynthetic active radiation absorbed by vegetation; and PAR is incident photosynthetic active radiation on the top of vegetation.

Because the photosynthetic rate decreases at low and high temperature, the effect of temperature on assimilation can be expressed as below:

$$f_1(T) = \frac{1}{(1 + e^{4.5-T})(1 + e^{T-37.5})} \quad (3)$$

Effect of soil water content on assimilation is

$$f_2(\beta) = 0.2 + 0.8\beta \quad (4)$$

and β is determined by the equation below:

$$\beta = \min\left(\frac{w_i}{w_k}, 1\right) \quad (5)$$

where w_i is soil water content in i month (mm); w_k is soil water content (mm) when evapotranspiration rate changes from potential rate unlimited by soil water to rate limited by soil water, it is about 70%-80% of field water-holding capacity w_{FC} ^[13]. We select w_k value as 75% of w_{FC} in the model.

Monthly soil water content is computed according to precipitation and potential evapotranspiration. When soil water content exceeds field capacity, the water over w_{FC} runs off. So soil water content in i month can be expressed as:

$$w_i = \min[(w_{i-1} + P_i - ET_{ai}), w_{FC}] \quad (6)$$

$$ET_{ai} = \beta \times ET_{pi} \quad (7)$$

where P_i is precipitation; ET_a and ET_p are actual and potential evapotranspiration in that month (mm). Potential evapotranspiration is computed by Penman's equation^[14]. w_{FC} is determined according to soil texture.

PAR is part of incident solar radiation and is computed using climate data^[15]:

$$PAR = 0.47Q \quad (8)$$

$$Q = Q_0(a_0 + b_0 \frac{n}{N}) \quad (9)$$

where Q is incident solar radiation. Q_0 is maximum incident solar radiation in sunny days, which is computed by latitude, altitude and vapor pressure; n/N is percentage of sunshine; a_0 and b_0 are empirical coefficients.

FPAR is calculated by the equation below^[16]:

$$FPAR = \frac{(SR - SR_{i,\min})(FPAR_{\max} - FPAR_{\min})}{(SR_{i,\max} - SR_{i,\min})} + FPAR_{\min} \quad (10)$$

where $FPAR_{\max}$ is maximum value of FPAR when land surface is fully covered by vegetation, $FPAR_{\min}$ is minimum value when ground surface is not covered by vegetation at all. $FPAR_{\max}=0.950$,

$FPAR_{min}=0.001$. SR is simple ratio. $SR_{i,max}$ and $SR_{i,min}$ are SR value when FPAR reaches maximum or minimum value for vegetation type i . SR can be derived from NDVI ($SR=(1+NDVI)/(1-NDVI)$). The max and min NDVI values for different vegetation types are listed in Table 1.

Table 1 Vegetation types and their parameters

Type	Vegetation	NDVI _{max}	NDVI _{min}	DW (gC/m ²)	R _{m0} (d ⁻¹)
a	Needle-leaved evergreen forest	0.689	0.039	10000	0.000208
b	Needle-leaved deciduous forest	0.689	0.039	10000	0.000208
c	Mixed needle-leaved and broad-leaved forest	0.721	0.039	20000	0.000208
d	Broad-leaved deciduous forest	0.721	0.039	20000	0.000208
e	Broad-leaved evergreen forest	0.611	0.039	20000	0.000208
f	Deciduous scrub	0.674	0.039	4000	0.000792
g	Evergreen scrub	0.674	0.039	4000	0.000792
h	Steppe	0.611	0.039	600	0.002083
i	Meadow	0.611	0.039	600	0.002083
j	Desert	0.674	0.039	200	0.002083
k	One crop per annum	0.674	0.039	600	0.002083
l	Two crops per annum	0.674	0.039	600	0.002083
m	Double cropping rice followed by a cool-loving crop per annum	0.674	0.039	600	0.002083
n	Double cropping rice followed by a thermophilous crop per annum	0.674	0.039	600	0.002083

Plant respiration includes maintenance respiration and growth respiration. Many studies proved that maintenance respiration rate will double when temperature increases 10°C [6]. In the model, maintenance respiration (R_m) is expressed as below

$$R_{m1} = DW \cdot R_{m0} Q_{10}^{(T-T_0)/10}$$

$$R_{m2} = \frac{NDVI}{NDVI_{max}} \cdot DW \cdot R_{m0} Q_{10}^{(T-T_0)/10} \quad (11)$$

where R_{m1} is daily maintenance respiration of forest and scrub (gC/m²d), R_{m2} is maintenance respiration of grassland and crop (gC/m²d), DW is dry weight of vegetation (gC/m²), Q_{10} is respiration coefficient, which equals to 2.0, $T_0=20$ °C, and R_{m0} is maintenance respiration coefficient (d⁻¹). The dry weight of different vegetation types is specified because it is difficult to determine. The values are listed in Table 1.

Growth respiration (R_g) is independent of temperature, it equals to

$$R_g = \gamma(GPP - \sum R_m) \quad (12)$$

where R_g is growth respiration (gC/m²month); $\sum R_m$ is monthly respiration; γ equals to 0.25^[17].

3.2 Model structure

NPP model includes 4 sub-models: gross primary productivity, respiration, radiation and soil water content. Figure 1 is the structure diagram of NPP model. Land surface net radiation and incident PAR are computed using latitude, altitude, vapor pressure and percentage of sunshine in radiation sub-model. Then soil texture, wind speed, precipitation and net radiation are imported into soil water content sub-model to compute evaporation ratio β . FPAR are computed from monthly NDVI image. Then PAR, evaporation ratio, FPAR and monthly mean air temperature are input to gross primary productivity sub-model, and monthly GPP are calculated. Plant respiration is estimated from vegetation type, air temperature and GPP.

Finally, subtract respiration wastage from GPP, we get monthly NPP and annual NPP.

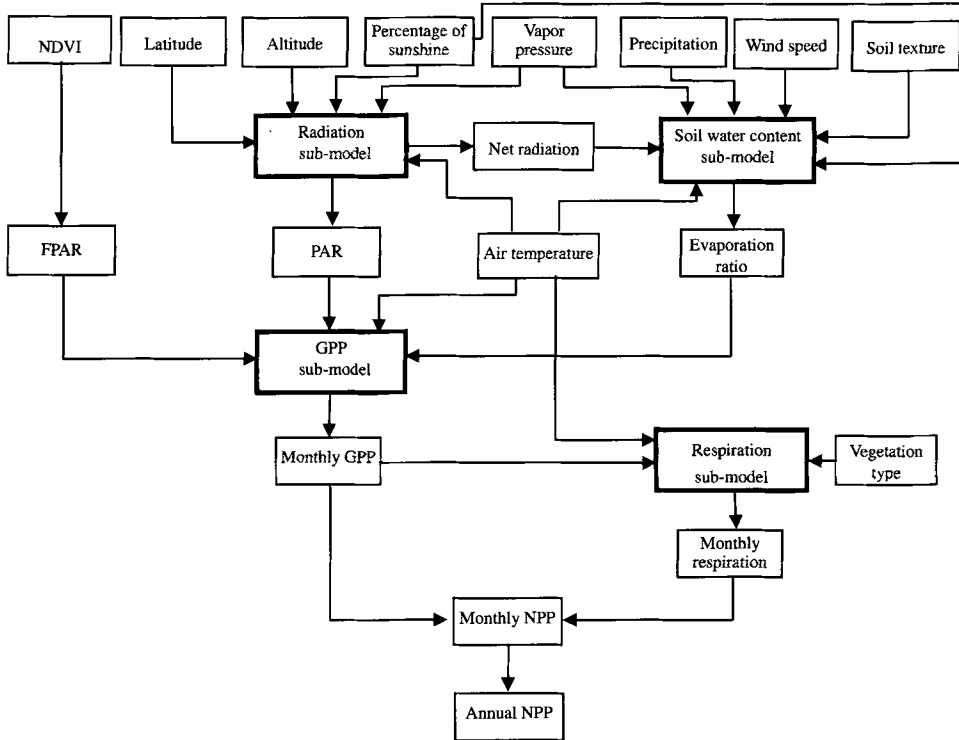


Figure 1 Structure diagram of net primary productivity model

4 Results and discussion

Using the model we developed and AVHRR NDVI data, we compute monthly and annual NPP in China. Meanwhile, Miami model is also used to estimate NPP in order to compare two results.

The total annual NPP in China computed by AVHRR NDVI is 2.645×10^9 tC while the result computed by Miami model is 7.438×10^9 tDW. Considering the ratio of dry matter weight and carbon weight is 0.5 approximately, then the total NPP estimated by Miami model is 3.719×10^9 tC. Our result is about 28.9% less than the Miami's. Due to the fact that Miami model doesn't consider land cover condition and its result is potential NPP, our result may be more close to truth.

4.1 Distribution of annual NPP in China

From the spatial distribution of annual NPP in China (Figure 2) we can know that, affected by moisture and temperature, NPP decreases from southeast to northwest. In sub-tropical zone, NPP of natural vegetation is above $500 \text{ gCm}^{-2}\text{a}^{-1}$, while NPP of most natural vegetation except some forest vegetation is less than $500 \text{ gCm}^{-2}\text{a}^{-1}$ in temperate zone. Because the natural vegetation is rain forest or evergreen broad-leaved forest in provinces of Hainan, Taiwan, southwest of Yunnan and some mountainous areas in Southeast China, NPP is very high. The NPP value is above $1,000 \text{ gCm}^{-2}\text{a}^{-1}$ and in some areas NPP exceeds $1500 \text{ gCm}^{-2}\text{a}^{-1}$. NPP is less than $100 \text{ gCm}^{-2}\text{a}^{-1}$ in arid and semiarid area. In desert area, NPP is less than $30 \text{ gCm}^{-2}\text{a}^{-1}$, the lowest amongst the others. From the image, we can also find that NPP in the plain area is lower than that of the surrounding mountainous areas. The reason is that the vegetation in the plain area is a crop while vegetation in the hill area is forest.

The calculated and observed NPP of different vegetation is listed in Table 2. NPP calculated by Miami model were also listed in the table.

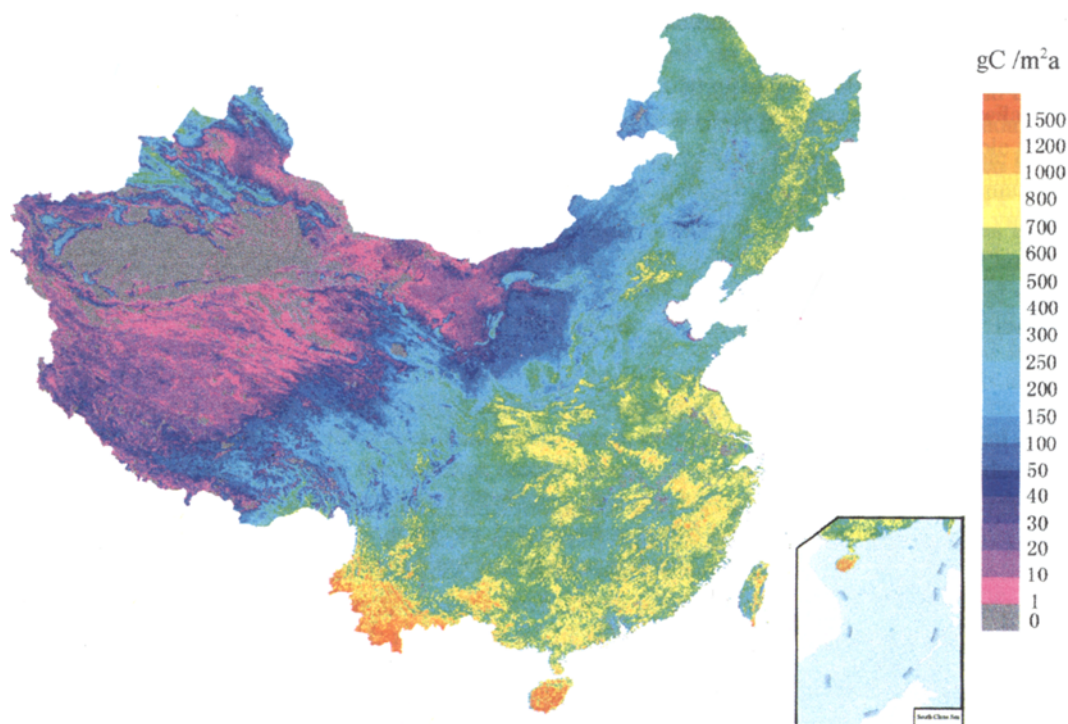


Figure 2 Spatial distribution of annual net primary productivity in China

Table 2 Annual net primary productivity of different types of vegetation ($\text{gCm}^{-2}\text{a}^{-1}$)*

Vegetation type	NPP calculated by NDVI data	NPP calculated by Miami model	Observed NPP
a	529.40	688.59	160-680 ^[18]
b	419.86	281.36	150-500 ^[18]
c	402.89	402.20	250-1000 ^[18]
d	459.70	440.68	250-700 ^[18]
e	971.90	751.15	910-1340 ^[18]
f	290.17	316.22	
g	555.42	778.98	
h	116.03	277.43	66-118 ^[19]
i	191.41	312.50	150-240 ^[120,21]
j	15.74	118.16	
k	313.31	372.39	
l	396.36	497.89	
m	496.87	783.34	
n	574.56	891.49	

* Because NPP is calculated by Miami model and observed data are dry matter weight, a conversion factor of 0.5 is used to convert them into carbon weight

From the table, we can know that the result using remote sensing data is more close to observed data.

There exist bigger errors between NPP calculated by Miami model and observed. The results show that NPP of broad-leaved evergreen forest and needle-leaved deciduous forest calculated by Miami model is smaller than ours; NPP of needle-leaved deciduous forest calculated by Miami model is about 30% smaller than ours. While for other vegetation types, the results of Miami model are higher than ours; among which, the difference of desert is the biggest, and it is 6 times higher than ours.

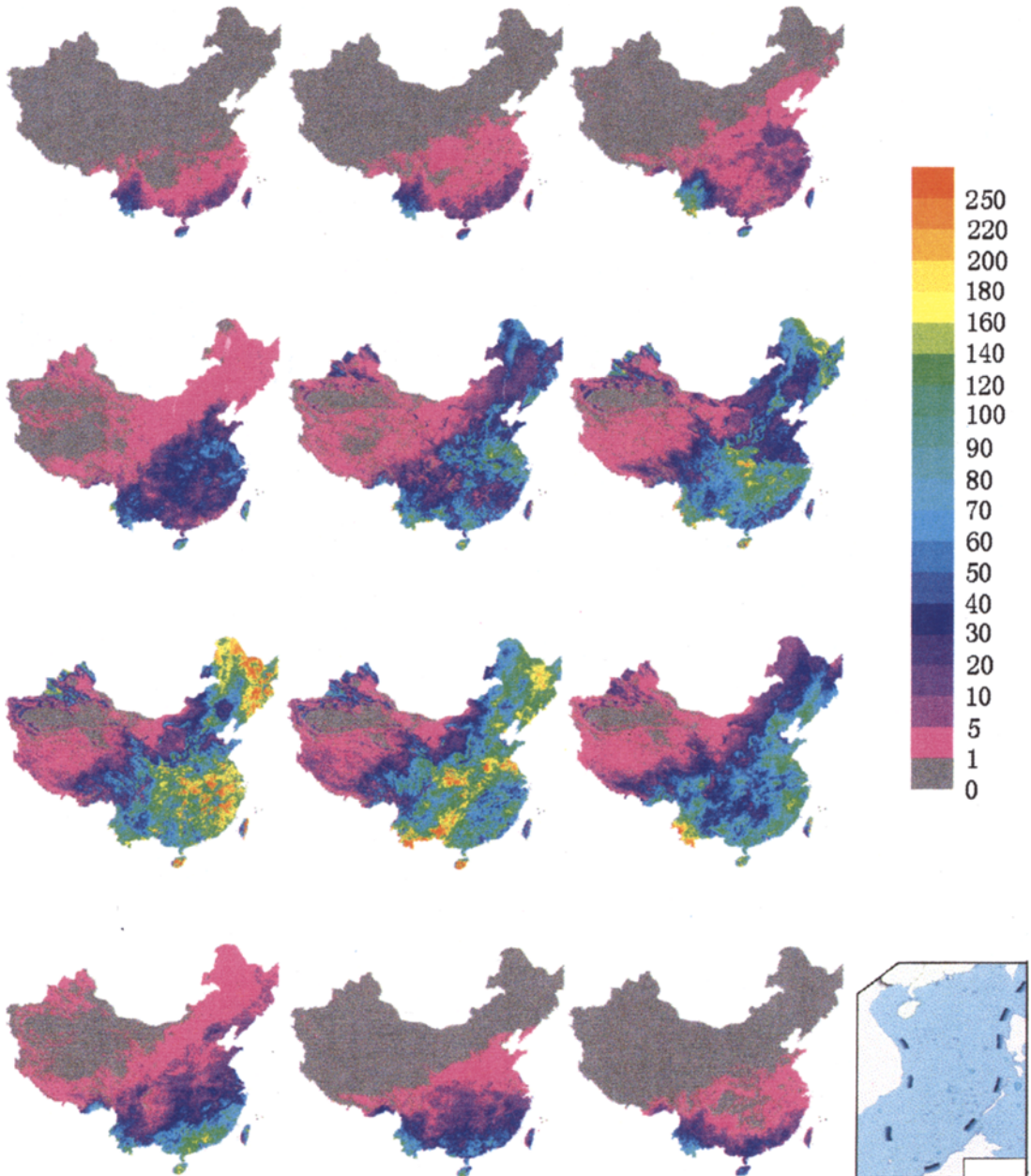


Figure 3 Seasonal change of monthly NPP in China

4.2 Seasonal change of NPP in China

Monthly NPP in China from April 1992 to March 1993 are showed in Figure 3. The image shows that the seasonal change of NPP is similar to that of temperature. NPP reaches to maximum value in summer when solar radiation reaches maximum, and NPP decreases to minimum in winter. Take January as an example, vegetation in most places stop growing and NPP equals to zero; only in south of Yunnan Province and southernmost of Hainan Island, NPP is greater than 50 gCm⁻². In July, NPP is greater than 100 gCm⁻² in most areas, but in part of desert area and non-vegetation area it is less than 10 gCm⁻².

The low and high NPP regions also change with season. The area that NPP equals to zero shrinks from north to Yangtze River in January to desert area in Northwest China in July. As for high NPP area, it lies in coastal zone of South China and Yunnan Province from January to March, and moves to Yangtze River and Huaihe River region in April and May. High NPP area moves from South China and mountainous area of Northeast China to East China between June and August. From the image we can also see that NPP is relatively low in North China Plain in June, it is because the first crops are harvested in this month.

Figure 4 shows the seasonal change of NPP of different vegetation. From the figure we can know that the seasonal change scope of NPP decreases from forest, scrub, crop, grassland to desert. Seasonal change of needle-leaved evergreen forest is the smallest among forest vegetation. For needle-leaved deciduous forest, its growth duration is the shortest and NPP changes sharply; NPP equals to zero from November to March and reaches maximum of 170 gCm⁻² in July. As for broad-leaved evergreen forest, max NPP appears in August, this is because it is rainy and the incident solar radiation is small in June and July.

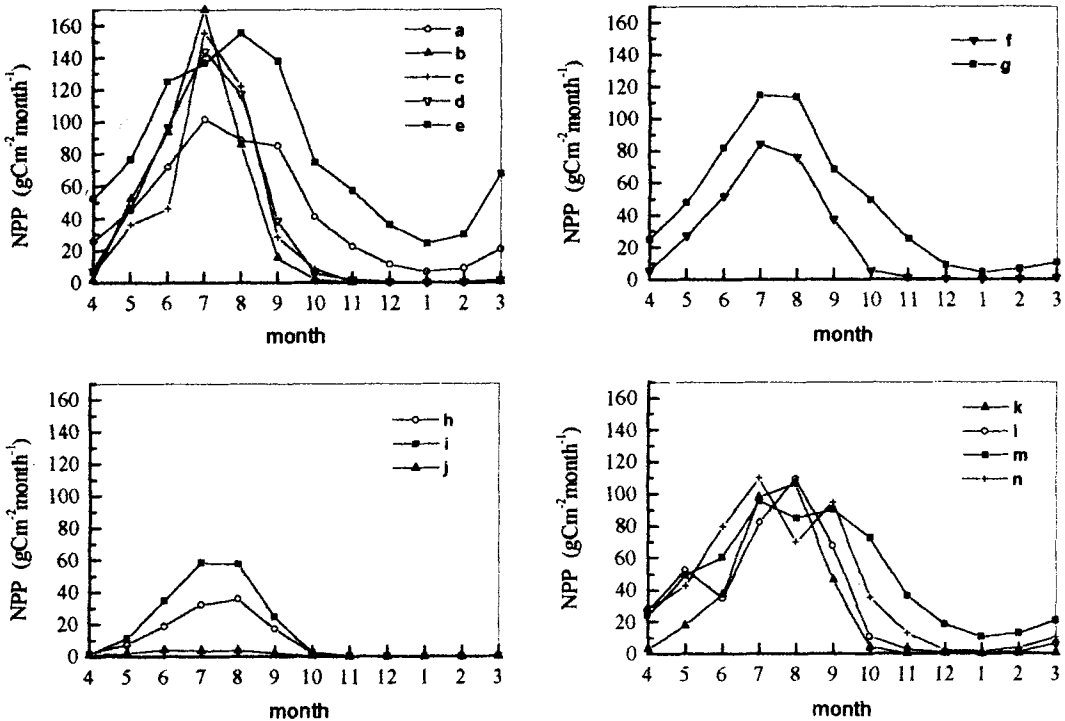


Figure 4 Seasonal change of NPP for different vegetation types

For scrub and grassland, NPP of evergreen scrub is higher than deciduous scrub. The meadow's NPP is also higher than the steppe's. We should point out that although the maximum value of steppe also

appears in August, the reason is different from broad-leaved needle forest. It is because in steppe region, rainy season is from end of July to August and the way that grass is growing is best in this season. In desert area, growth of plant is limited by moisture condition, vegetation is very sparse and its NPP is the lowest.

For crop vegetation, there are two NPP climaxes for some types of crops. For example, in regions of two crops per annum, the first climax is in May and the second one is in August. Because crop is harvested in June, NPP is small. It also shows that the first climax is lower than the second one. The reason is that the first main crop is wheat and the second is corn, and the productivity of wheat is lower than that of corn.

5 Conclusion

Remote sensing technology enables us to observe land surface on a large scale repeatedly. It reflects not only the status quo, but also the change procession of land surface. Therefore, remote sensing has been a useful tool to monitor ground net productivity and biomass. In this paper, an NPP model using remotely sensed data has been developed, and 1km resolution AVHRR NDVI data and climate data are used to study spatial distribution and seasonal change of NPP in China. The results show that NPP estimated by remotely sensed data is more close to ground truth. The total annual terrestrial NPP in China is $2.645 \times 10^9 \text{tC}$ and NPP is high in southeast region and low in northwest. NPP is above $500 \text{gCm}^{-2}\text{a}^{-1}$ in most of subtropical zone while it is below $30 \text{gCm}^{-2}\text{a}^{-1}$ in desert area. The maximum NPP value appears in Hainan and southwest of Yunnan provinces.

References

- [1] Sun Rui, Zhu Qijiang. Net primary productivity of terrestrial vegetation: a review on related researches. *Chinese Journal of Applied Ecology*, 1999, **10**(6): 757-760.
- [2] Lieth H, Whittaker R H. Primary Productivity of the Biosphere. New York: Springer-Verlag, 1975.
- [3] Zhu Zhihui. A model for estimating net primary productivity of natural vegetation. *Chinese Science Bulletin*, 1993, **38**(15): 1422-1426.
- [4] Zhou Guangsheng, Zhang Xinshi. Study on NPP of natural vegetation in China under global climate change, *Acta Phytocologica Sinica*, 1996, **20**(1): 11-19.
- [5] Liu J, Chen J M, Cihlar J *et al.* A process-based boreal ecosystem productivity simulator using remote sensing inputs. *Remote Sensing of Environment*, 1997, **62**(2): 158-175.
- [6] Foley J A. Net primary productivity in the terrestrial biosphere: the application of a global model. *J. Geophys. Res.*, 1994, **99**(D10): 20773-20783.
- [7] Running S W, Coughlan J C. A general model of ecosystem processes for regional applications I: hydrologic balance, canopy gas exchange and primary production processes. *Ecological Modelling*, 1988, **42**: 125-154.
- [8] Potter C S, Randerson J T *et al.* Terrestrial ecosystem production: a process model based on global satellite and surface data. *Global Biogeochemical Cycles*, 1993, **7**(4): 811-841.
- [9] Ruimy A, Saugier B. Methodology for the estimation of terrestrial net primary production from remotely sensed data. *J. Geophys. Res.*, 1994, **99**(D3): 5263-5283.
- [10] Prince S D, Goward S N. Global primary production: a remote sensing approach. *Journal of Biogeography*, 1995, **22**: 815-835.
- [11] Eidenshink J C, Faundeen J. L. The 1km AVHRR global land dataset: first stages in implementation. *Int. J. Remote Sensing*, 1994, **15**: 3443-3462.
- [12] Deng Shiqin. Map of Soil Texture of China. In: Institute of Soil Science, Academia Sinica. The Soil Atlas of China. Beijing: Cartographic Publishing House, 1986. 23-24.
- [13] Milly P C D. Potential evaporation and soil moisture in general circulation models. *Journal of Climate*, 1992, **5**(3): 209-226.
- [14] Wang Yixian. Tables for quick computation of the Penman estimation of potential evapotranspiration. *Geographical Research*, 1983, **2**(1): 93-107.
- [15] Hou Guangliang, Li Jiyong, Zhang Yiguang. Agroclimate Resources in China. Beijing: Renmin University Press

- of China, 1993.
- [16] Sellers P J, Tucker C J, Collatz G J et al. A global 1° by 1° NDVI data set for climate studies part 2: the generation of global fields of terrestrial biophysical parameters from the NDVI. *Int. J. Remote Sensing*, 1994, **15**(17): 3519-3545.
- [17] Hunt E R. Relationship between woody biomass and PAR conversion efficiency for estimating net primary production from NDVI. *Int. J. Remote Sensing*, 1994, **15**: 1725-1730.
- [18] Liu Shirong, Xu Deying, Wang Bing. Impacts of climate change on productivity of forests in China I: geographic distribution of actual productivity of forests in China. *Forest Research*, 1993, **6**(6): 634-642.
- [19] Wang Yifeng. The biomass and productivity of typical steppe in Inner Mongolia. *Plants*, 1993, (4): 10-11.
- [20] Hu Zizhi, Sun Jixiong, Zhang Yinsheng et al. Studies on primary productivity in Tianzhu alpine *Polygonum Viviparum* meadow I: biomass dynamics and conversion efficiency for solar radiation. *Acta Phytoecologica et Geobotanica Sinica*, 1988, **12**(2): 123-133.
- [21] Yang Futun, Wang Qiji, Shi Shunhai. The allocation of the biomass and energy in *Kobresia Humilis* meadow, Haibei district, Qinghai Province. *Acta Phytoecologica et Geobotanica Sinica*, 1987, **11**(2): 106-112.